

# Highly Directive Planar End-Fire Antenna Array

Sruthi Dinesh<sup>1, \*</sup>, Chalu V. Vinisha<sup>1</sup>, Deepti D. Krishna<sup>1</sup>,  
Jean M. Laheurte<sup>2</sup>, and Chandroth K. Aanandan<sup>1</sup>

**Abstract**—This paper describes the design and development of a highly directive planar end-fire array using arc dipoles as the array elements. The inter element spacing, shape, and size of the array elements are optimized for maximum directivity and gain. The array is printed on a substrate whose dimensions are also optimized for better performance. The overall length of the proposed six element array is  $1.9\lambda$ , giving directivity and gain values as 12.0 dBi and 10.2 dB respectively at 5.8 GHz.

## 1. INTRODUCTION AND BACKGROUND

The development of super-directive antennas has been enthralling the research community for over decades, primarily owing to the difficulties encountered during their practical realization such as low gain and efficiency. It is well known that by modifying the shape and spacing between the parasitic and driven elements, it is possible to attain higher directivity than that of conventional end-fire arrays [1, 2]. Compact directive arrays find applications in RFID, remote control, or as an element for a larger array with beam steering capability for point-to-multipoint or point-to-point connections such as the line linking the base station and a mobile equipment [3].

An antenna whose directivity is higher than the directivity of the uniformly excited aperture with the same physical size or the normal directivity defined by Harrington [4] is termed as super-directive. Different methods are reported to get enhanced directivity such as decreasing the inter-element spacing [5], adjusting the current distribution by applying excitation coefficients of Schelkunoff or Tschebyscheff polynomials [6, 7], exciting adjacent elements with calculated optimal current excitation coefficients [8], employing metamaterials [9–12] or using properly loaded parasitic elements [13–16] or a combination of these methods. Many of these designs reported low efficiency, gain and poor impedance matching [14–16].

In this paper, we present the design of a highly directive planar array with good gain, impedance matching, bandwidth, and efficiency. The novelty of our work lies in the fact that we have been able to attain better directivity by adjusting parameters like shape, inter element spacing, number of array elements, and substrate dimensions which play an important role in the antenna performance. Each parameter gives a small increase in directivity without deteriorating the impedance matching. The design is done in a step by step process, and the cumulative result is an antenna with better gain and a relatively smaller size. The obtained directivity and gain values are greater than that provided by similar arrays already reported as demonstrated in Table 1.

The proposed planar dipole array comprises a driven element, a parasitic reflector element, and four directors. Simulations are done using CST Microwave Studio.

In our earlier work, we have demonstrated the performance of a two element array on a trapezoid-shaped substrate [17]. Here in this work, aiming at a better gain, a detailed study of the different

---

*Received 8 August 2020, Accepted 17 September 2020, Scheduled 6 October 2020*

\* Corresponding author: Sruthi Dinesh (sruthidinesh11@cusat.ac.in).

<sup>1</sup> Department of Electronics, Cochin University of Science and Technology, India. <sup>2</sup> ESYCOM Laboratory, Université Gustave Eiffel, CNRS, F-77454 Marne-la-Vallée, France.

**Table 1.** Comparison of proposed antenna with other structures.

Structures	Number of elements, Array Length	Directivity (dBi)
Ordinary end-fire array [1, p. 280]	10 elements, $2.25\lambda$	$(4Nd/\lambda) = 10$
[18]	20 elements, $17.7\lambda$	19.2
[19]	12 elements, $3.7\lambda$	10
[20]	6 elements, $2.25\lambda$	11.7
[21]	15 elements, $4.6\lambda$	11.3
[22]	8 elements, $2.54\lambda$	11.7
	10 elements, $3.18\lambda$	12.4
Proposed antenna	6 elements, $1.9\lambda$	12

parameters for optimum performance of a six element array is presented. For the ease of fabrication and measurement, we have tested the concept at 5.8 GHz. Table 1 shows a comparison between the proposed work and a few related publications. As observed, results have been improved while considering the size factor and the corresponding directivity values.

## 2. ARRAY DESIGN

The antenna array is designed using a driven arc dipole and five parasitic arc dipoles, as arc dipoles provide higher directivity than straight dipoles. In this section, the details of the design, such as the individual element size, shape, substrate parameters, and arrangement of array elements, are described. The analysis is started with straight dipoles and then extended to arc dipoles. Initially, arc lengths, arc radii, and inter element spacing of reflector and driven element are optimized for better directivity without deteriorating the impedance matching. This is followed by the optimization of substrate dimensions. Finally, directors are added in the extended substrate. Here also, the parameters are optimized as described in the following sections. The cumulative result is an antenna with better gain and a relatively smaller size. The design described here is for 5.8 GHz, which can be scaled to any frequency. Of course, fine tuning will be required which has to be done by simulation.

### 2.1. Array Element: Dipole

#### 2.1.1. Straight Dipole

The driven element is a near-half-wave centre-fed planar dipole on an FR4 dielectric substrate as shown in Figure 1. The dimension of the substrate is chosen as  $40 \times 40 \text{ mm}^2$ , which is more than one wavelength in the dielectric ( $\lambda_g$ ) at the design frequency of 5.8 GHz ( $\lambda = 51.7 \text{ mm}$ ,  $\epsilon_r = 4.4$ ,  $\epsilon_{r\text{eff}} \approx (\epsilon_r + 1)/2 = 2.7$ ,  $\lambda_g = \lambda/\sqrt{\epsilon_{r\text{eff}}} = 31.5 \text{ mm}$ ). The length  $l$  and width  $w$  of the dipole element are chosen as 18 mm and 3 mm respectively to obtain resonance at 5.8 GHz. Since the aim is to construct an end-fire array whose radiation maximum is along the array axis, the effect of the position of the dipole on the substrate is also investigated.

From simulations, it is observed that dipole placed at the edge of the substrate gives a better directivity of 2.88 dBi than that at the middle of the substrate which has a directivity of 2.32 dBi at 5.8 GHz. The return loss curve for dipole at the edge of the substrate is given in Figure 2.

#### 2.1.2. Arc Dipole

Here, the dipole is bent in the form of an arc to see the improvement in the performance.

The effect of arc radius on  $S_{11}$  and directivity is studied keeping the length of the arc equal to that of the straight dipole, that is  $l = 18 \text{ mm}$ , and the observations are plotted. For arc dipole, there is

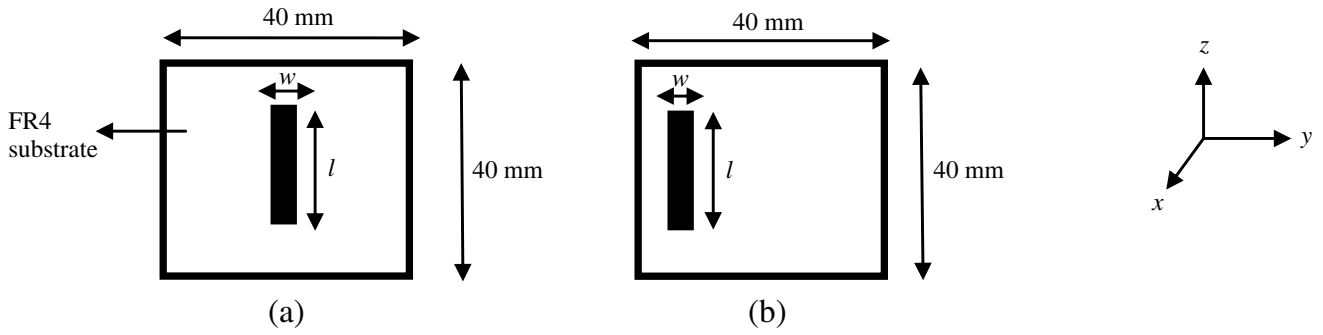


Figure 1. Planar straight dipole on FR4 substrate, (a) dipole at the middle, (b) dipole at the edge.

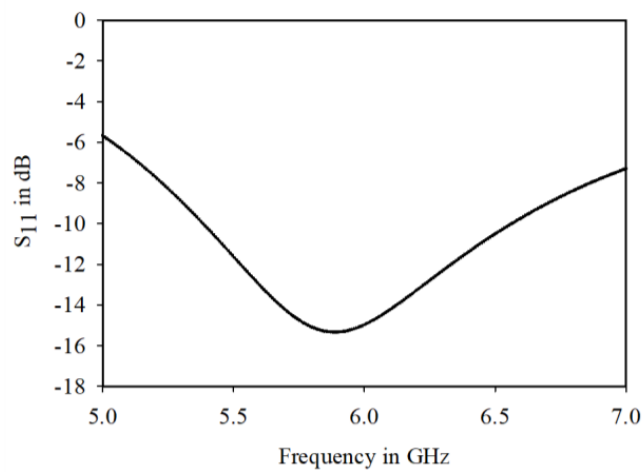


Figure 2. Return loss curve for the dipole at substrate edge.

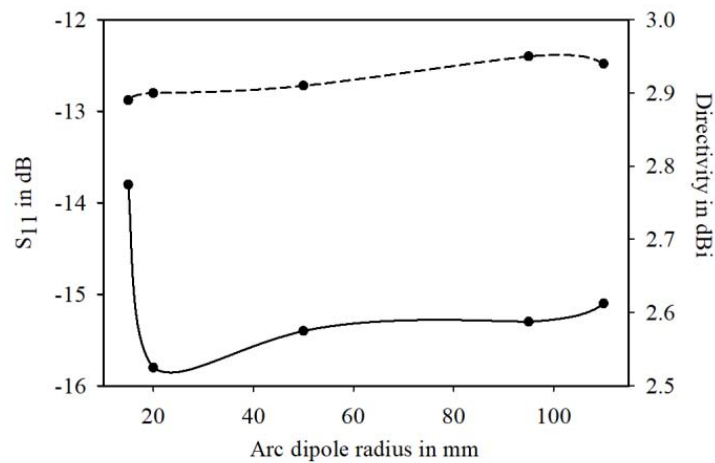


Figure 3. Effect of arc dipole radius (—  $S_{11}$ , - - - Directivity).

an optimum radius which gives higher directivity than a straight dipole. Here 95 mm is the optimum radius which gives a better directivity of 2.95 dBi with a return loss of 15.3 dB as shown in Figure 3.

## 2.2. Addition of Parasitic Element

### 2.2.1. Straight Parasitic Dipole of Equal Length

Here a parasitic dipole of length equal to that of the driven dipole is placed adjacent to it. It is well known that a parasitic element kept near a driven element will modify the directivity. The excitation amplitude and phase of the parasitic element mainly depend upon the spacing. As inter element spacing decreases below  $0.5\lambda$ , directivity keeps increasing till  $0.1\lambda$ . If spacing is reduced below  $0.1\lambda$ , directivity decreases. Optimum directivity is found to exist between  $0.125\lambda$  and  $0.1\lambda$ . Here in this case, the spacing for maximum directivity is  $0.121\lambda$  or 6.25 mm. But as spacing decreases to  $0.125\lambda$  and less, impedance matching and gain deteriorate. Here, the lengths of the dipoles are adjusted to 16.5 mm so that the resonance of the combination is at 5.8 GHz.

Electric field distributions for a two element array, with one parasitic dipole (left) and one driven dipole (right) separated by  $0.5\lambda$  and reduced optimized spacing  $0.121\lambda$  in substrate of dimension 40 mm by 40 mm are illustrated in Figures 4(a) and 4(b), respectively.

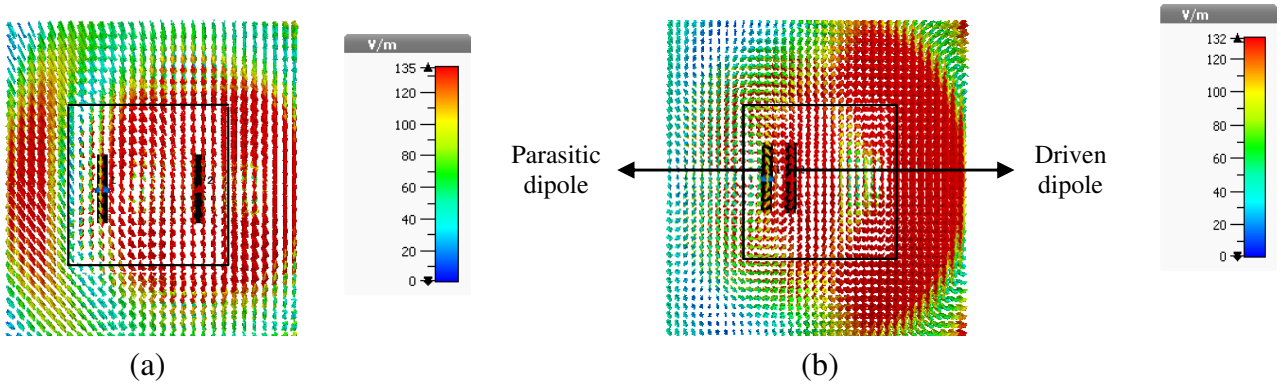


**Figure 4.** Electric field distribution for two straight parasitic dipoles at (a)  $0.5\lambda$  spacing, (b)  $0.121\lambda$  spacing.

As seen from the figures, fields are spread towards both directions when the spacing between dipoles is  $0.5\lambda$  or 25.85 mm. But when spacing decreases to 6.25 mm, fields are more concentrated towards one direction due to the relative excitation phase. But as spacing decreases, impedance matching deteriorates even though directivity is increased. To attain impedance matching, the length of the parasitic element has to be increased.

### 2.2.2. Straight Parasitic Dipole of Different Length

Length of the driven element is 16.5 mm. Length of the parasitic element is adjusted so that maximum directivity is obtained without compromising impedance matching. As seen from Figure 5, the optimum length of shorted parasitic element which gives maximum directivity of 6.85 dBi with good return loss of 11.6 dB is 19 mm.

So it can be concluded that while driven and parasitic dipoles of equal length 16.5 mm give a directivity of 6.35 dBi with poor matching, parasitic dipole with adjusted length 19 mm along with the driven element of length 16.5 mm gives high directivity of 6.85 dBi without compromising impedance matching. The matching can be observed from the Smith chart in Figure 6.

## 2.3. Optimization of Two Arc Dipoles

Having optimized the lengths and spacing of straight dipoles, we find the optimum radii and lengths of two arc dipoles for improved directivity and impedance matching.

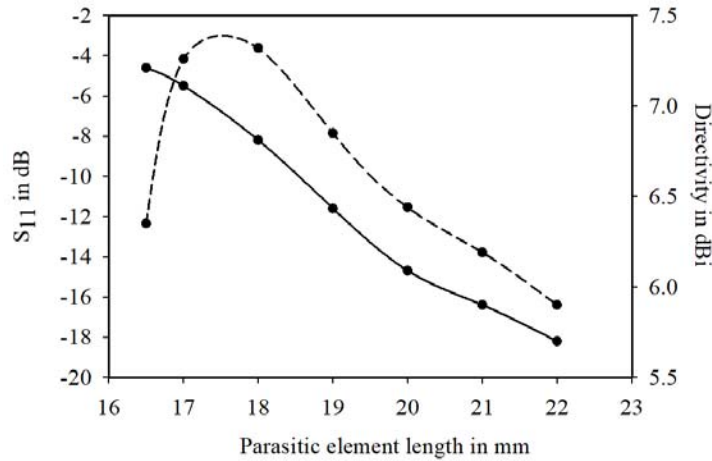


Figure 5. Effect of parasitic element length of straight dipole (—  $S_{11}$ , - - - Directivity).

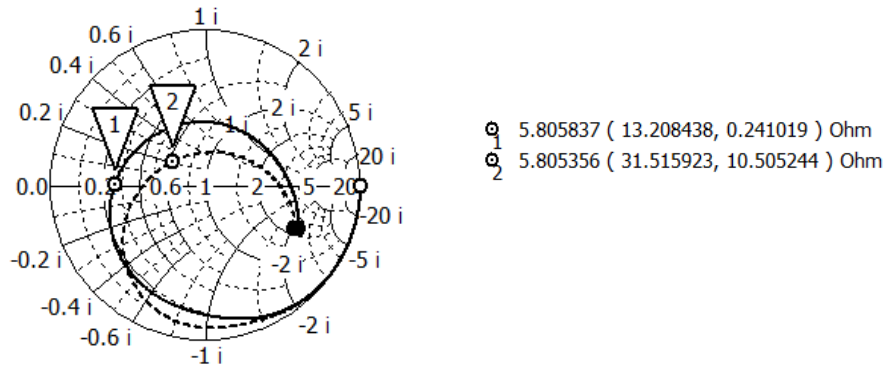


Figure 6. Smith Chart for (— two equal length dipoles, - - - two dipoles with optimized lengths).

2.3.1. Effect of Arc Radius of Parasitic Element

To find the optimum radius for parasitic dipole, the arc length of driven element is chosen as 16.5 mm, and its arc radius is 95 mm as optimized before. Length of the parasitic element is kept the same as that of the value obtained for straight dipole, that is, 19 mm. Simulation is done for different arc radii of parasitic element, and the observations are shown in Figure 7.

The optimum arc radius of parasitic element which gives maximum directivity is taken as 100 mm. So the combination of parasitic and driven elements with arc radii of 100 mm and 95 mm respectively provide a pattern of directivity 6.91 dBi with a return loss of 12.1 dB.

2.3.2. Optimization of Arc Dipole Parasitic Element Length

Now for these arc radii, we studied the effect of inter-element spacing and length on the directivity. For the optimum arc radius of 100 mm, the effect of arc length of parasitic element on return loss and directivity is illustrated in Figure 8.

It can be observed that the optimum arc length of parasitic element which gives the maximum directivity of 6.94 dBi without compromising impedance matching is 19.2 mm. It can also be seen from the graph that we can get a higher value of directivity with a reduced matching. The inter-element spacing for arc dipoles is also optimized to 6.34 mm (0.122λ) to get this directivity value as shown in Figure 9.

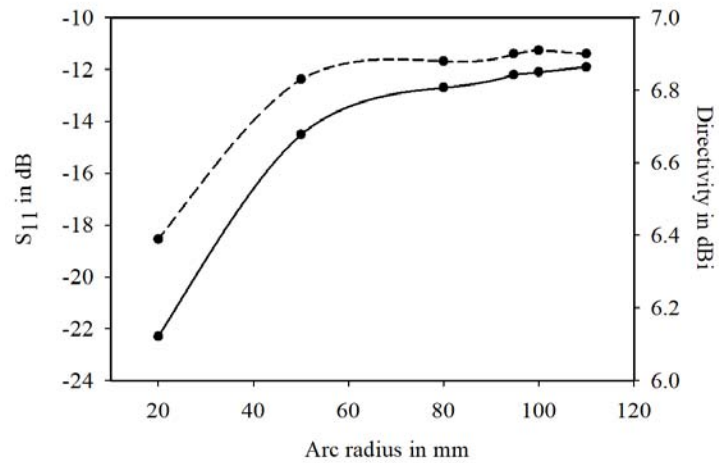


**Figure 7.** Effect of arc radius of parasitic element (—  $S_{11}$ , - - - Directivity).

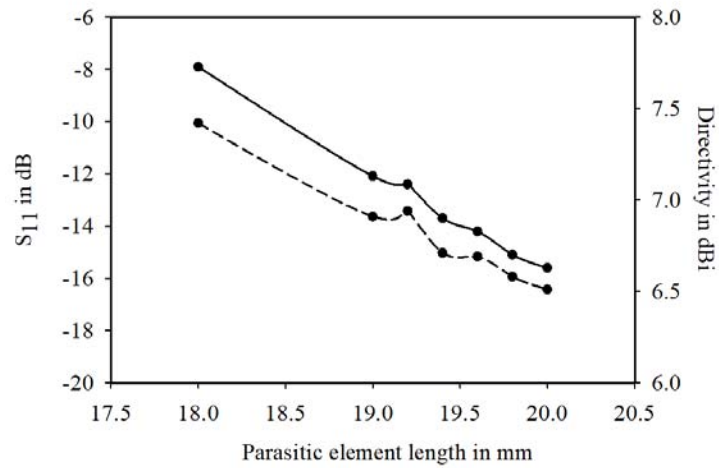


**Figure 8.** Effect of arc length of parasitic element (—  $S_{11}$ , - - - Directivity).

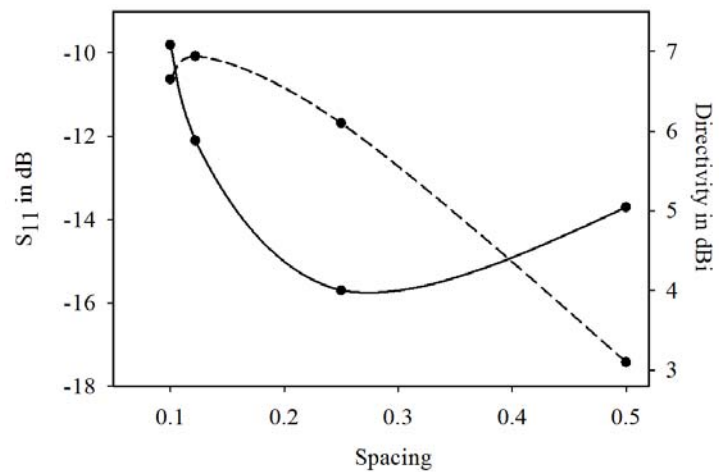


**Figure 9.** Effect of inter-element spacing of arc dipoles (—  $S_{11}$ , - - - Directivity).

### 2.4. Effect of Substrate Dimension

Having optimized the arc radii, arc length, and spacing, a study is conducted to analyze the effect of substrate dimensions on directivity.

#### 2.4.1. Effect of Substrate Length

Substrate dimensions in all the studies conducted till now were 40 mm by 40 mm. Now the substrate length is extended, and the effect on directivity is observed from Figure 10.

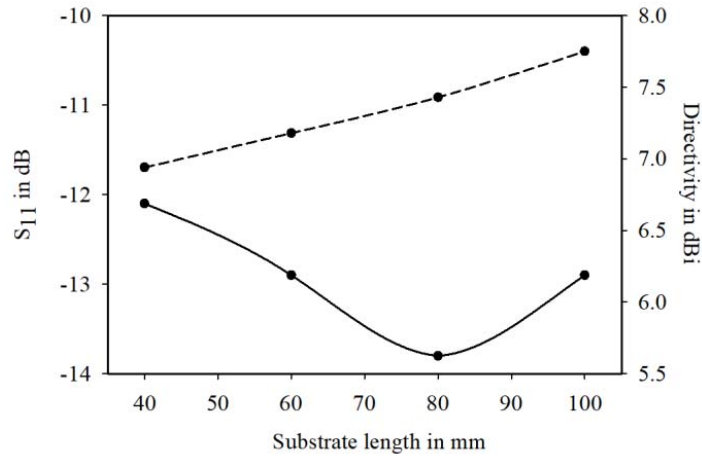


**Figure 10.** Effect of substrate length (—  $S_{11}$ , - - - Directivity).

When the substrate width is fixed at 40 mm, directivity keeps increasing as the substrate length is increased normal to the dipole arms. This is because the equivalent radiating surface becomes large. So we take an optimum length of 100 mm which gives a directivity of 7.75 dBi with a return loss of 12.9 dB. Further increase in length deteriorates the impedance matching.

#### 2.4.2. Effect of Substrate Width

Now the effect of substrate width on directivity is studied by keeping the length fixed at 40 mm, and observations are illustrated in Figure 11.

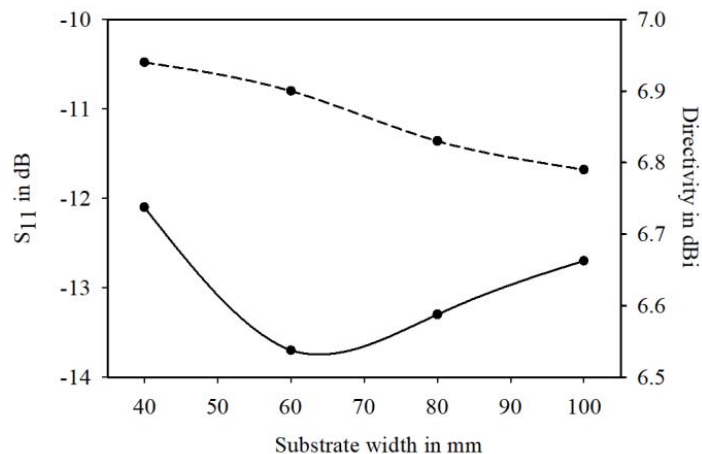


**Figure 11.** Effect of substrate width (—  $S_{11}$ , - - - Directivity).

It is observed that extending the substrate width does not give any improvement in directivity. So the substrate dimensions are selected as 40 mm by 100 mm as shown in Figure 12.

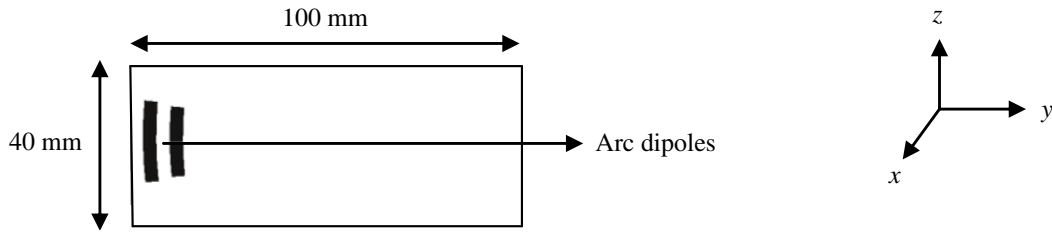


Figure 12. Arc dipoles on extended substrate.

### 2.5. Effect of Flaring on Directivity

The effect of flaring on substrate directivity is also analyzed by varying the widths of left and right edges of the rectangle to form a trapezoidal shape. Initially, the width of left edge is fixed at 40 mm, substrate length fixed at 100 mm, and the width of right edge is changed to observe the effect on directivity.

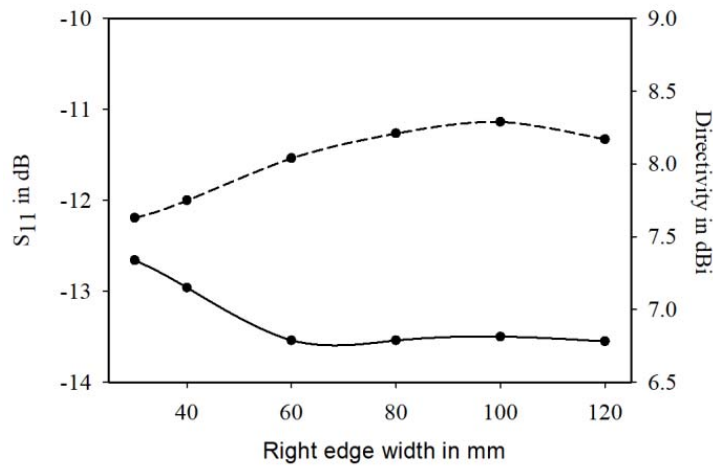


Figure 13. Effect of variation of right edge width (—  $S_{11}$ , - - - Directivity).

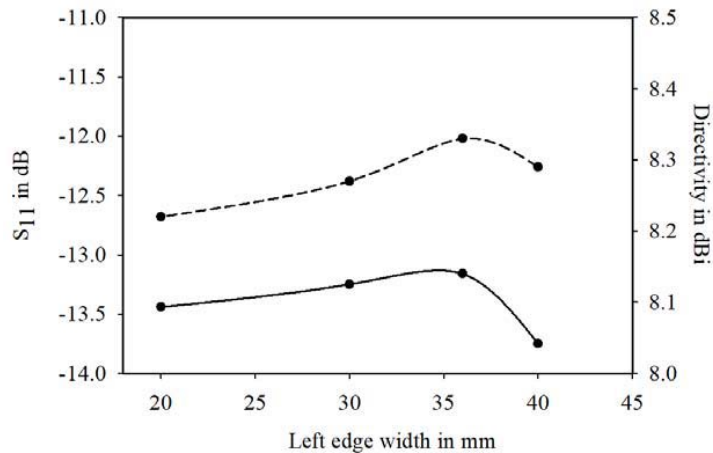


Figure 14. Effect of variation of left edge width (—  $S_{11}$ , - - - Directivity).



The observations are depicted in Figure 13. So if the flaring or width of right edge is increased, directivity increases up to an optimum width of 100 mm. If the width is increased beyond 100 mm, directivity decreases. So the width of right edge is chosen as 100 mm which gives a directivity of 8.29 dBi with a return loss of 13.5 dB. Now keeping the width of right edge fixed at 100 mm, the width of left edge is decreased to check if there is any improvement in directivity, and the observations are shown in Figure 14.

It is observed that the maximum directivity of 8.33 dBi with a return loss of 13.2 dB is obtained when the width of left edge is 36 mm, and that of right edge is 100 mm. Beyond this optimum value, if the width of right edge is increased or that of left edge is reduced, directivity decreases. So the optimized dimensions of the trapezoidal substrate are left edge of width 36 mm ( $0.7\lambda$ ), right edge of width 100 mm ( $1.9\lambda$ ) and array length as 100 mm ( $1.9\lambda$ ).

### 2.6. Addition of Directors

Now in the extended substrate, arc directors of optimum radii are added to improve directivity without compromising impedance matching. Upon addition of the first director at approximately  $0.122\lambda$  from the driven element, previously attained impedance matching is affected. When the second director is placed at  $0.24\lambda$  from the first director, impedance matching is restored. So two directors are added initially without affecting the previously attained impedance matching. Length and arc radii of two arc directors are optimized to get the maximum directivity.

#### 2.6.1. Optimization of Director Length

Initially the arc curvature is taken similar to that of driven and parasitic elements, and the arc length of directors is optimized. Observations are shown in Figure 15. So the arc length of directors which gives maximum directivity of 10.2 dBi without compromising impedance matching is 13.5 mm.

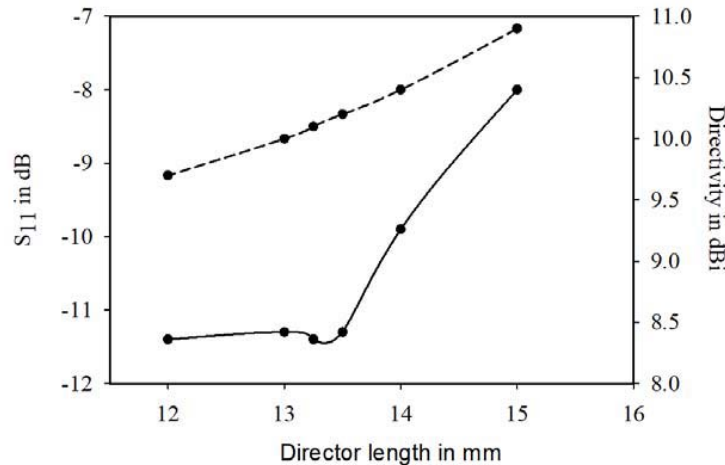


**Figure 15.** Effect of director arc length (—  $S_{11}$ , - - - Directivity).

#### 2.6.2. Optimization of Director Arc Radius

Here arc length is taken as 13.5 mm, and the optimization of arc radius is done for two directors. The effect of variation of arc radius is shown in Figure 16.

So the optimum arc radius of directors giving maximum directivity of 10.7 dBi without compromising impedance matching is obtained as 10 mm.

Having done the optimization of arc length and radius for two directors, more directors are added in the extended substrate to enhance the directivity without affecting the already attained impedance

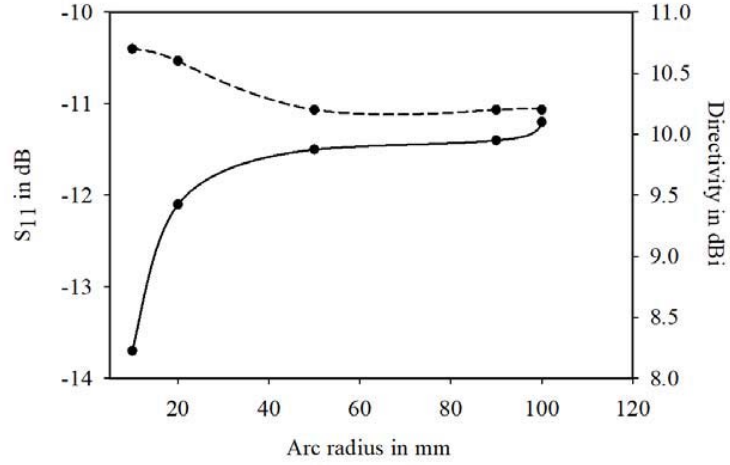


**Figure 16.** Effect of director arc radius (—  $S_{11}$ , - - - Directivity).

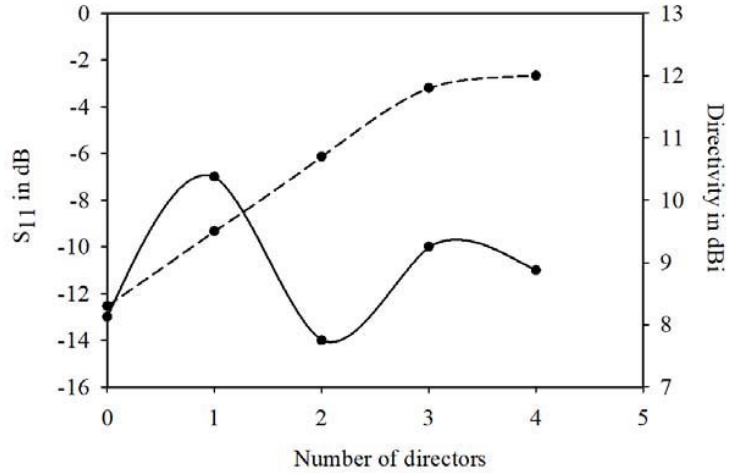


**Figure 17.** Effect of addition of directors (—  $S_{11}$ , - - - Directivity).

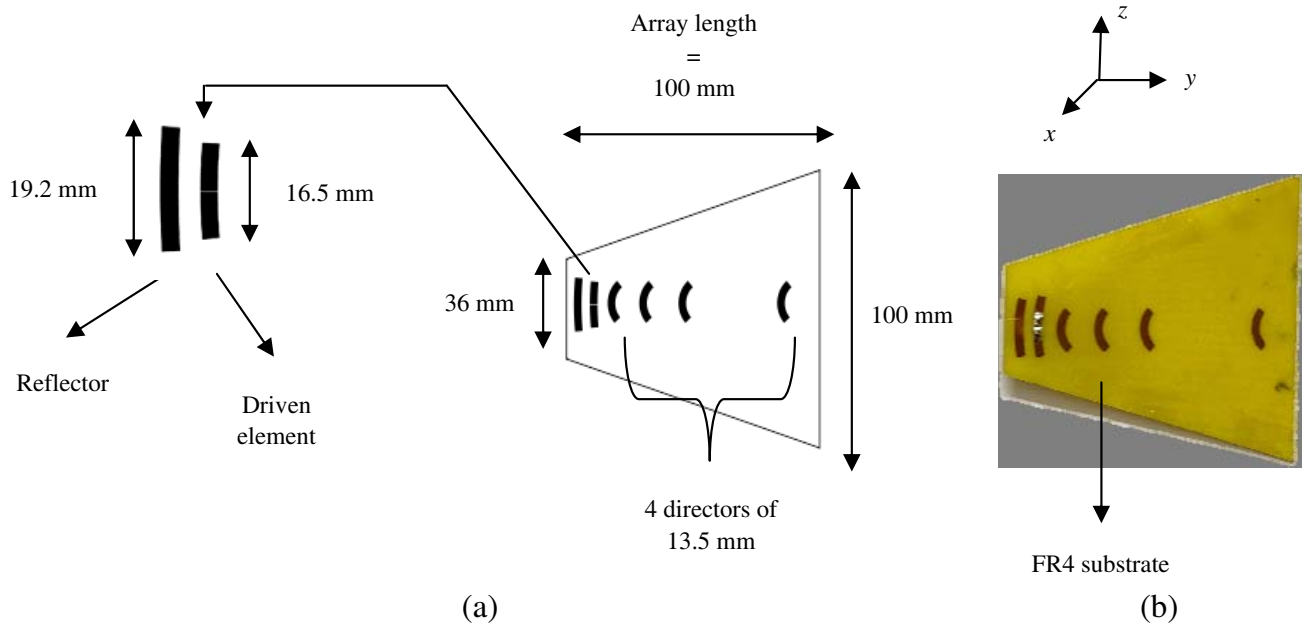
matching. The third and fourth directors are added at a distance of approximately  $0.3\lambda$  and  $0.75\lambda$  from their previous directors.

Figure 17 shows the progressive increase in directivity with the addition of each director element. With the addition of all four directors, the simulated directivity is 12 dBi, and simulated gain is 11 dB with a realized gain of 10.6 dB at 5.8 GHz.

Thus we have optimized a highly directive antenna with two edges of widths 36 mm and 100 mm, array length as 100 mm, and the reflector, driven element and director lengths as 19.2 mm (greater than  $\lambda_g/2$ ), 16.5 mm (approximately  $\lambda_g/2$ ) and 13.5 mm (less than  $\lambda_g/2$ ) respectively where  $\lambda_g$  is the guided wavelength in the dielectric. The schematic and fabricated prototype of the proposed antenna are shown in Figures 18(a) and 18(b).

### 3. PRINCIPLE OF THE PROPOSED ANTENNA

An arc dipole of optimum radius can provide higher directivity than straight dipole. As inter-element spacing between two straight or two arc dipoles decreases from  $0.5\lambda$  to around  $0.12\lambda$ , directivity increases. Directivity is initially optimized for two elements, that is, reflector and driven element, and finally directors are added in the extended substrate.



**Figure 18.** (a) Schematic and (b) fabricated prototype of the proposed antenna.

The analysis of a two element structure has been done in our earlier work [17]. Initially the two element array is considered as fully driven, and current excitation coefficients for maximizing the directivity are calculated using Yaghjian optimization method [8] for different inter-element spacings. The two element fully driven array at optimum spacing is then converted to a parasitic array which gives almost the same directivity as the fully driven array. The optimal load to be connected to the parasitic element is determined with the help of calculated current excitation coefficients and  $Z$ -matrix of the two element array obtained from CST simulation results [13]. It was found that loading a capacitance of suitable value could give maximum directivity. Shorting the parasitic element also gave equivalent results, probably because the capacitor behaves like a short at high frequencies.

So shorted parasitic element of length equal to that of the driven element is placed at a distance of  $0.122\lambda$  to obtain maximum directivity. But as impedance matching is affected in this case, the length of parasitic element is increased which subsequently acts as a reflector. So a shorted parasitic element approximately  $0.1\lambda_g$  longer than driven element, placed  $0.15\lambda$  to  $0.12\lambda$  from the driven element produces highly directive beams in the end-fire direction besides satisfactory impedance matching, gain, and bandwidth. Extending the substrate width and flaring gives higher directivity as the equivalent radiating surface becomes large. Directors of optimum radii, length, and spacing, placed in the extended substrate, further contribute to directivity.

#### 4. SIMULATED AND MEASURED RESULTS

Antenna is fabricated by photolithographic technique, and measurements of the fabricated prototype are performed with Agilent E8362B PNA.

Figure 19(a) illustrates simulated and measured VSWRs, and Figure 19(b) depicts the measured gain for the proposed antenna. The driven dipole has been fed using an SMA connector in such a way that signal pin is connected to one arm of the dipole, and ground pin is connected to the other arm of the dipole. In this design, we have not incorporated any balun. The problem of unbalanced currents arising due to feeding balanced dipole by unbalanced coaxial cable can be solved by using ferrite toroid or similar structures.

The simulated VSWR is 1.4 at 5.8 GHz, and the measured VSWR is 1.2. The measured 2 : 1 VSWR bandwidth is 400 MHz extending from 5.7 GHz to 6.1 GHz which matches the simulated result. Using the gain comparison method, the maximum measured gain is 10.2 dB at 5.8 GHz. Measured gain

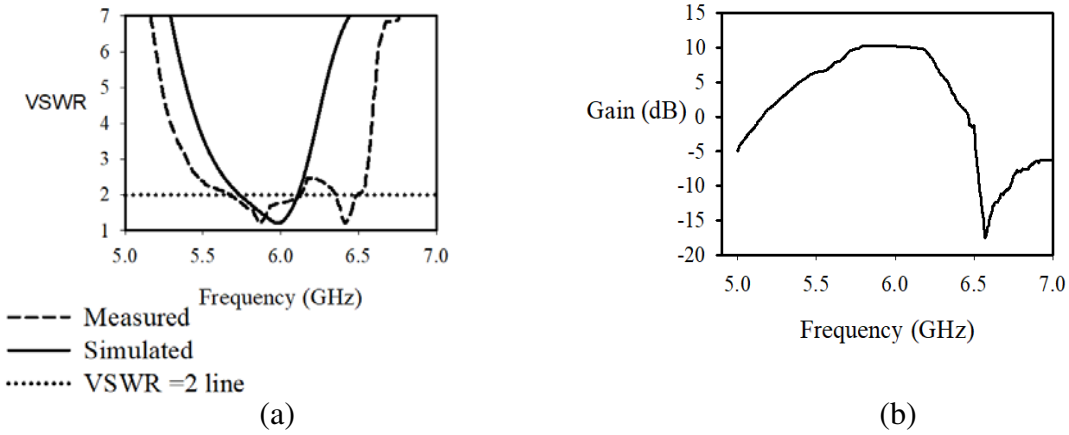


Figure 19. (a) Simulated and measured VSWR. (b) Measured gain.

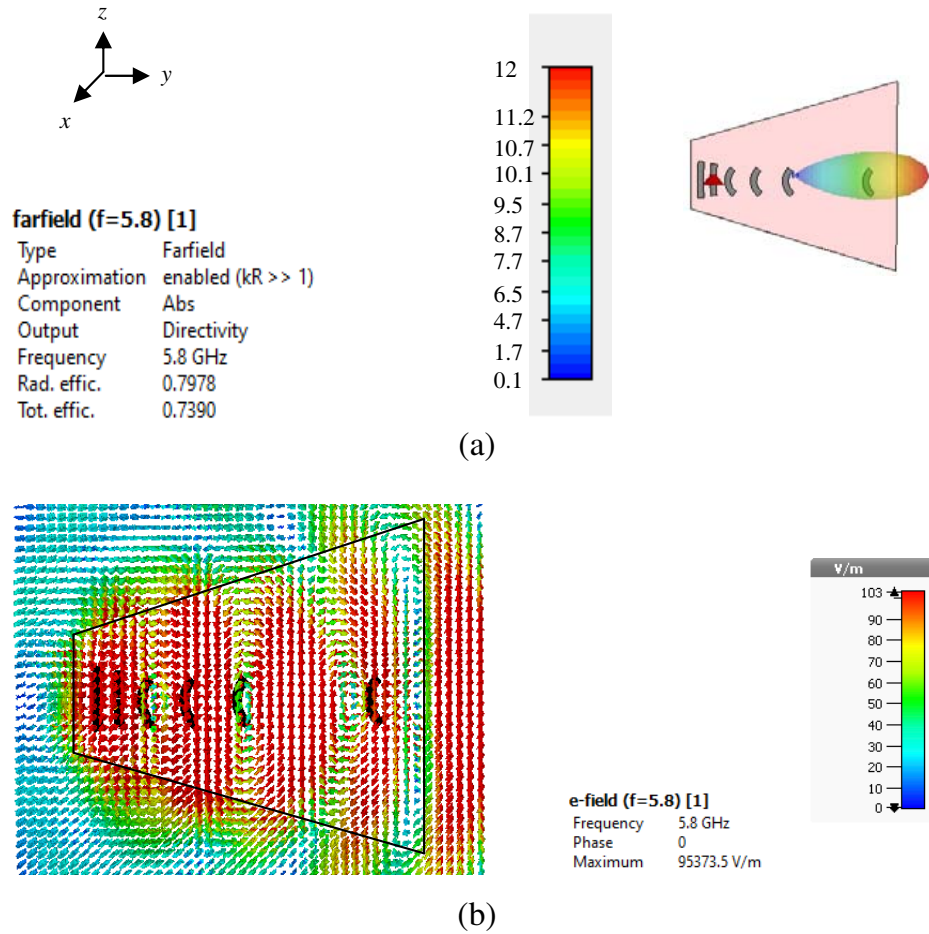


Figure 20. (a) Simulated 3D radiation pattern. (b) Electric field distribution.

varies from 9.5 to 10.2 dB in the frequency band. The additional measured resonance at 6.4 GHz could be due to the presence of multiple elements and fabrication tolerances, but the gain is very low at this frequency as seen from Figure 19(b).

Figures 20(a) and 20(b) show the simulated 3D patterns and the electric field distribution of the proposed antenna, respectively. Simulated directivity varies from 11.5 to 12 dBi, and simulated gain

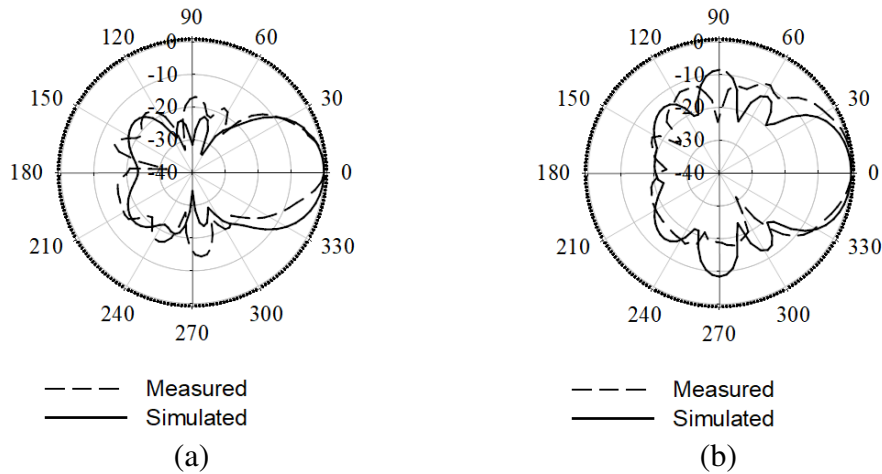


Figure 21. Co-polar patterns (a)  $E$  plane, (b)  $H$  plane.

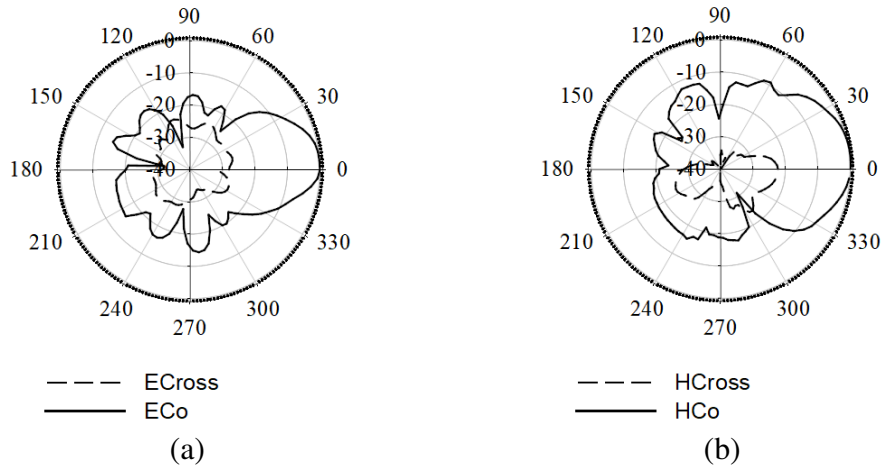


Figure 22. Measured co-polar and cross-polar patterns (a)  $E$  plane, (b)  $H$  plane.

varies from 9.6 to 11 dB in the frequency band. The 2D patterns are measured in an anechoic chamber. Figures 21(a) and 21(b) illustrate the simulated and measured 2D co-polar patterns in the  $E$  plane ( $YZ$ ) and  $H$  plane ( $XY$ ) of the antenna respectively at 5.8 GHz. The measured patterns shown in Figures 22(a) and 22(b) indicate that the cross polar levels are very low.

Based on the Wheeler cap method [23], a 70% efficiency  $\eta$  is measured using  $\eta = R_r / (R_r + R_L)$ , with  $R_r$  as the radiation resistance and  $R_L$  as the loss resistance, and simulated efficiency is 74%. Simulated and measured side-lobe levels in  $E$ -plane are  $-17$  dB and  $-15$  dB, respectively. The simulated and measured side-lobe levels in  $H$ -plane are around  $-10$  dB.

The measured half-power beamwidth at 5.8 GHz is  $52^\circ$  in the  $H$ -plane ( $\theta_H$ ) and  $40^\circ$  in the  $E$ -plane ( $\theta_E$ ).  $\theta_H$  varies from  $48^\circ$  to  $55^\circ$ , and  $\theta_E$  varies from  $40^\circ$  to  $48^\circ$  in the frequency band. Using the approximate formula of directivity [1],  $D = 32400 / (\theta_H \theta_E) = 32400 / (52^\circ 40^\circ) = 15.6$  or  $11.9$  dBi, which is close to the simulated value.

In all our parametric studies leading to the final optimized structure, we have studied the effect of parameters on  $S_{11}$  and directivity to ensure that the enhancement in directivity does not affect the impedance matching. Only those values have been chosen where  $S_{11}$  value is less than  $-10$  dB which corresponds to a VSWR value less than 2. In our final optimized structure, we have attained a VSWR value well below 2 at the resonant frequency besides a directivity of 12 dBi in the end-fire direction. We have also measured the gain, bandwidth, and efficiency which were found to be satisfactory.

## 5. CONCLUSION

A highly directive planar endfire array comprising a driven element and five parasitic arc dipoles capable of providing radiation patterns of directivity 12 dBi and realized gain of 10.2 dB has been designed and fabricated. The geometry of the elements and the dimensions and shape of the substrate have been optimized for maximum directivity. The conventional problems associated with super-directive arrays such as low gain, bandwidth, and efficiency have been overcome in the proposed design. Satisfactory impedance matching, gain, radiation efficiency, and bandwidth are attained.

## ACKNOWLEDGMENT

The authors would like to acknowledge SERB for supporting the project under VAJRA scheme and UGC for providing financial assistance through research fellowship and CSIR for the support through Emeritus Scientist scheme.

## REFERENCES

1. Balanis, C. A., *Antenna Theory: Analysis and Design*, 2nd edition, John Wiley and Sons Inc., 1997.
2. Hansen, R. C. and R. E. Collin, *Chapter 6: Superdirective Antennas, Small Antenna Handbook*, John Wiley and Sons Inc., 2011.
3. Siachalou, E., E. Vafiadis, S. S. Goudos, T. Samaras, C. S. Koukourlis, and S. Panas, "On the design of switched-beam wideband base stations," *IEEE Antennas and Propagation Magazine*, Vol. 46, No. 1, 158–167, Feb. 2004.
4. Harrington, R. F., "Effect of antenna size on gain, bandwidth and efficiency," *Journal of Research of the National Bureau of Standards — D. Radio Propagation*, Vol. 64D, No. 1, 1–12, Jan.–Feb. 1960.
5. Uzkov, A. I., "An approach to the problem of optimum directive antenna design," *C.R. Dold, Acad. Sci. USSR*, Vol. 53, No. 1, 35–38, 1946.
6. Schelkunoff, S. A., "A mathematical theory of linear arrays," *The Bell System Technical Journal*, Vol. 22, No. 1, 80–107, Jan. 1943.
7. Dolph, C. L., "A current distribution for broadside arrays which optimises the relationship between beamwidth and side-lobe level," *Proceedings of the IRE*, Vol. 34, No. 6, 335–348, Jun. 1946.
8. Altshuler, E. E., T. H. O'Donnell, A. D. Yaghjian, and S. R. Best, "A monopole superdirective array," *IEEE Transactions on Antennas and Propagation*, Vol. 53, No. 8, 2653–2661, Aug. 2005.
9. Pirhadi, A. and M. Hakkak, "An analytical investigation of the radiation characteristics of infinitesimal dipole antenna embedded in partially reflective surfaces to obtain high directivity," *Progress In Electromagnetics Research*, Vol. 65, 137–155, 2006.
10. Pajewski, L., L. Rinaldi, and G. Schettini, "Enhancement of directivity using 2D electromagnetic crystals near the band-gap edge: A full-wave approach," *Progress In Electromagnetics Research*, Vol. 80, 179–196, 2008.
11. Abbaspour-Tamijani, A., L. Zhang, and H. K. Pan, "Enhancing the directivity of phased array antennas using lens-arrays," *Progress In Electromagnetics Research M*, Vol. 29, 41–64, 2013.
12. Radkovskaya, A., S. Kiriushchikina, A. Vakulenko, P. Petrov, L. Solymar, L. Li, A. Vallecchi, C. J. Stevens, and E. Shamonina, "Superdirectivity from arrays of strongly coupled meta-atoms," *Journal of Applied Physics*, Vol. 124, No. 10, 104901, 2018.
13. Haskou, A., A. Sharaiha, and S. Collardey, "Design of small parasitic loaded superdirective end-fire antenna arrays," *IEEE Transactions on Antennas and Propagation*, Vol. 63, No. 12, 5456–5464, Dec. 2015.
14. Hammoud, M., A. Haskou, A. Sharaiha, and S. Collardey, "Small end-fire superdirective folded meandered monopole antenna array," *Microwave and Optical Technology Letters*, Vol. 58, No. 9, 2122–2124, 2016.

15. Clemente, A., C. Jouanlanne, and C. Delaveaud, "Analysis and design of a four-element superdirective compact dipole antenna array," *2017 11th European Conference on Antennas and Propagation (EUCAP)*, 2700–2704, Paris, 2017.
16. Clemente, A., M. Pigeon, L. Rudant, and C. Delaveaud, "Design of a super directive four-element compact antenna array using spherical wave expansion," *IEEE Transactions on Antennas and Propagation*, Vol. 63, No. 11, 4715–4722, Nov. 2015.
17. Dinesh, S., D. D. Krishna, J. M. Laheurte, and C. K. Aanandan, "A super-directive two-element parasitic dipole antenna," *2019 IEEE Asia-Pacific Microwave Conference (APMC)*, 554–556, Singapore, 2019.
18. Yao, G.-W., Z.-H. Xue, W.-M. Li, W. Ren, and J. Cao, "Research on a new kind of high directivity end-fire antenna array," *Progress In Electromagnetics Research B*, Vol. 33, 135–151, 2011.
19. Liu, J. and Q. Xue, "Microstrip magnetic dipole Yagi array antenna with endfire radiation and vertical polarization," *IEEE Transactions on Antennas and Propagation*, Vol. 61, No. 3, 1140–1147, Mar. 2013.
20. Cai, X., W. Geyi, and H. Sun, "A printed dipole array with high gain and endfire radiation," *IEEE Antennas and Wireless Propagation Letters*, Vol. 16, 1512–1515, 2017.
21. Aguila, P., S. Zuffanelli, G. Zamora, F. Paredes, F. Martin, and J. Bonache, "Planar Yagi-Uda antenna array based on split-ring resonators (SRRs)," *IEEE Antennas and Wireless Propagation Letters*, Vol. 16, 1233–1236, 2017.
22. Guo, H. and W. Geyi, "Design of Yagi-Uda antenna with multiple driven elements," *Progress In Electromagnetics Research C*, Vol. 92, 101–112, 2019.
23. Choo, H., R. Rogers, and H. Ling, "On the wheeler cap measurement of the efficiency of microstrip antennas," *IEEE Transactions on Antennas and Propagation*, Vol. 53, No. 7, 2328–2332, Jul. 2005.